Mon. Not. R. Astron. Soc. **357,** 608–618 (2005) doi:10.1111/j.1365-2966.2005.08667.x

The two-point correlation of galaxy groups: probing the clustering of dark matter haloes

Xiaohu Yang,[1⋆] H. J. Mo,[1] Frank C. van den Bosch[2] and Y. P. Jing[3]

[1] *Department of Astronomy, University of Massachusetts, Amherst MA 01003-9305, USA*
[2] *Department of Physics, Swiss Federal Institute of Technology, ETH Hönggerberg, CH-8093, Zurich, Switzerland*
[3] *Shanghai Astronomical Observatory, the Partner Group of MPA, Nandan Road 80, Shanghai 200030, China*

Accepted 2004 November 23. Received 2004 November 16; in original form 2004 June 25

ABSTRACT

We analyse the two-point correlation function (2PCF) of galaxy groups identified from the 2-degree Field Galaxy Redshift Survey with the halo-based group finder recently developed by Yang et al. With this group catalogue we are able to estimate the 2PCFs for systems ranging from isolated galaxies to rich clusters of galaxies. The real-space correlation length obtained for these systems ranges from $\sim$4 to $\sim 15\,h^{-1}$ Mpc, respectively. The observed correlation amplitude (and the corresponding bias factor) as a function of group abundance is well reproduced by associating galaxy groups with dark matter haloes in the standard Λ-cold dark matter model. Redshift distortions are clearly detected in the redshift-space correlation function, the degree of which is consistent with the assumption of gravitational clustering and halo bias in the cosmic density field. In agreement with previous studies we find a strong increase of the correlation length with the mean intergroup separation. Although well-determined observationally, we show that current theoretical predictions are not yet accurate enough to allow for stringent constraints on cosmological parameters. Finally, we use our results to explore the power-law nature of the 2PCF of galaxies. We split the 2PCF into one- and two-group terms, equivalent to the one- and two-halo terms in halo occupation models, and show that the power-law form of the 2PCF is broken, when only including galaxies in the more massive systems.

Key words: methods: statistical – galaxies: haloes – dark matter – large-scale structure of Universe.

1 INTRODUCTION

In the standard cold dark matter (CDM) cosmogony galaxies are assumed to form in virialized dark matter haloes. Theoretically, the properties of the halo population can be studied in great detail with the use of high-resolution N-body simulations and sophisticated analytical models. Observationally, however, dark matter haloes can only be detected indirectly, either through their gravitational lensing of background sources, or by using galaxies and/or X-ray gas as tracers of the dark matter potential wells. In this paper we investigate the clustering of dark matter haloes using the second method.

Based on galaxy kinematics, X-ray studies and gravitational lensing effects, it is now well established that clusters of galaxies are associated with the most massive dark matter haloes. Observations show that clusters of galaxies are strongly clustered. The cluster–cluster two-point correlation function, $\xi_{\rm cc}(r)$, is roughly a power law, $\xi_{\rm cc}(r) = (r_0/r)^{\alpha}$, with $\alpha \sim 1.8$ and with a correlation length, r_0, that is much larger than that of galaxies (see Bahcall 1988 for a review; Croft et al. 1997; Park & Lee 1998; Bahcall et al. 2003). This is in good agreement with clusters being associated with massive dark matter haloes, which are expected to be strongly clustered from the fact that they are associated with high peaks in the initial density field (e.g. Kaiser 1984).

The correlation length of clusters is also observed to increase with the mean intercluster separation $d \equiv n^{-1/3}$, where n is the number density of objects (e.g. Bahcall & West 1992). As richer clusters (where richness expresses the number of galaxy members) are rarer objects, this relation between r_0 and d is equivalent to a relation between r_0 and cluster richness. Associating richer clusters with more massive haloes, this, again, is in good agreement with theoretical predictions. Mo, Jing & White (1996), using the halo bias model developed by Mo & White (1996), found that the observed r_0–d relation can be well described in terms of halo–halo correlation functions in the CDM cosmogony. In addition, these authors showed that the relation between correlation length and mean separation can be used to constrain models of structure formation. In particular, they showed that the observed r_0–d relation is well reproduced by a

⋆E-mail: xhyang@astro.umass.edu

ΛCDM model with $\Omega_{m,0} = 0.3$ and $h = 0.7$, but differs significantly from the predictions for a CDM model with $\Omega_{m,0} = 1$ and $h = 0.5$ (see also Bahcall et al. 2003).

The r_0–d relation for poorer systems can be probed by studying the correlation function of galaxy groups (Zandivarez, Merchan & Padilla 2003; Padilla et al. 2004). Using groups of galaxies selected from the 2-degree Field Galaxy Redshift (2dFGRS; Eke et al. 2004), Padilla et al. (2004) found that the s_0–d relation (with s_0 the correlation length in redshift space) obeyed by clusters extends to poor groups. Unfortunately, the connection between galaxy groups and dark matter haloes is less straightforward than for rich clusters, simply because the smaller number of galaxies involved in individual groups makes it harder to identify systems that are physically associated. The correspondence between galaxy groups and dark matter haloes may therefore depend significantly on the group finder used, complicating the interpretation of the observational results. In order to overcome this problem, one needs a group finder that associates galaxies according to their common dark matter haloes.

In a recent paper (Yang et al. 2004b, hereafter YMBJ), we developed a halo-based group finder that is optimized for grouping galaxies that reside in the same dark matter halo. We tested the performance of this group finder extensively using mock galaxy redshift surveys constructed from the conditional luminosity function model (van den Bosch, Yang & Mo 2003; Yang, Mo & van den Bosch 2003; Yang et al. 2004a), and found that our group finder is more successful than the conventional friends-of-friends (FOF) algorithm in associating galaxies according to their common dark matter haloes. In particular, our group finder also performs reliably for very poor systems, including isolated galaxies in small-mass haloes.

In this paper we analyse the two-point correlation function (2PCF) of the galaxy groups identified by YMBJ. As we will show, our group catalogue allows us to determine 2PCFs for vastly different systems, ranging from isolated galaxies to rich clusters. Using detailed mock galaxy redshift surveys (hereafter MGRSs), we show that the group correlation functions are closely related to those of dark matter haloes. The paper is organized as follows. In Section 2, we briefly describe our group finder, and summarize the properties of the group catalogues obtained from the 2dFGRS and the MGRSs. In Section 3 we estimate the 2PCF of galaxy groups in the 2dFGRS. The relation between the correlation of galaxy groups and that of dark matter haloes is examined in Section 4. In Section 5, we analyse how the correlation length of galaxy groups depends on the abundance of the systems under consideration, and we compare the observational results with theoretical predictions in Section 6. In Section 7, we use our results to discuss how one can understand the galaxy–galaxy correlation function in terms of the group–group correlation function and the galaxy occupation in groups. Finally, in Section 8, we summarize our results.

Unless stated otherwise, we consider a flat ΛCDM cosmology with $\Omega_m = 0.3$, $\Omega_\Lambda = 0.7$ and $h = H_0/(100\ \mathrm{km\ s^{-1}\ Mpc^{-1}}) = 0.7$ and with initial density fluctuations described by a scale-invariant power spectrum with normalization $\sigma_8 = 0.9$. All distances are calculated using this cosmology.

2 GALAXY GROUPS AND DARK MATTER HALOES

2.1 The group finder

In a recent study (YMBJ), we developed a halo-based group finder that can successfully assign galaxies into groups according to their common haloes. The basic idea behind our group finder is similar to that of the matched filter algorithm developed by Postman et al. (1996, see also Kepner et al. 1999; Kim et al. 2002; White & Kochanek 2002; Kochanek et al. 2003; van den Bosch et al. 2004a,b), although we also made use of the galaxy kinematics. In summary (see YMBJ for details), the group finder starts with an assumed mass-to-light ratio to assign a tentative mass to each potential group. This mass is used to estimate the size and velocity dispersion of the underlying halo that hosts the group, which in turn is used to determine group membership (in redshift space). This procedure is iterated until no further changes occur in group memberships (see the Appendix for more details). We tested the performance of our group finder in terms of the completeness of true members and contamination by interlopers, using detailed MGRSs. The average completeness of individual groups is ∼90 per cent and with only ∼20 per cent interlopers. Furthermore, the resulting group catalogue is insensitive to the initial assumption of the mass-to-light ratios, and the group finder is more successful than the conventional FOF method (Eke et al. 2004) in associating galaxies according to their common dark matter haloes.

2.2 2dF groups and mock catalogues

In YMBJ we applied the group finder described above to the final public data release of the 2dFGRS. This observational sample contains 250 000 galaxies with redshifts and is complete to an extinction-corrected apparent magnitude of $b_J \approx 19.45$ (Colless et al. 2001). The survey volume of the 2dFGRS consists of two separate declination strips in the North Galactic Pole (NGP) and the South Galactic Pole (SGP), respectively, together with 100 2-degree fields spread randomly in the southern Galactic hemisphere. When identifying galaxy groups, we restricted ourselves only to galaxies with redshifts $0.01 \leqslant z \leqslant 0.20$ in the NGP and SGP regions. Only galaxies with a redshift quality parameter of $q \geqslant 3$ and with a redshift completeness of >0.8 were used. This left a total of 151 280 galaxies with a sky coverage of 1124 deg^2. We obtained a group catalogue of 78 708 systems, which in total contain 104 912 galaxies. Among these systems, 7251 are binaries, 2343 are triplets and 2502 are systems with four or more members. However, the vast majority of the groups (66 612 systems) in our catalogue consist of only a single member. Note that some faint galaxies are not assigned to any systems, because it is difficult to decide if they are either the satellite galaxies of larger systems, or if they are the central galaxies of small haloes.

As discussed in YMBJ, it is not reliable to estimate the (total) group luminosity based on the assumption that the galaxy luminosity function in groups is similar to that of field galaxies. We therefore used a more empirical approach to estimate the group luminosity L_{18}, defined as the total luminosity of all group members brighter than $M_{b_J} - 5\log h = -18$. In the Appendix we describe in detail how L_{18} is estimated for each group. As demonstrated in detail in YMBJ, L_{18} is tightly correlated with the mass of the dark matter halo hosting the group, and can be used to rank galaxy groups according to halo masses. Fig. 1 plots the redshift distributions of groups detected in the 2dFGRS (solid dots) and in our MGRSs (open circles). The solid line corresponds to a constant number density, and is shown for comparison. As already shown in YMBJ, the group catalogue is virtually complete over the entire redshift range ($0.01 \leqslant z \leqslant 0.20$) for groups with $L_{18} > 10^{10.5}\,h^{-2}\,\mathrm{L}_\odot$ (right-hand panel). For groups with smaller L_{18}, the catalogue is incomplete: groups with $10^{10} < L_{18} < 10^{10.5}\,h^{-2}\,\mathrm{L}_\odot$ are only complete to $z \sim 0.13$ (middle panel), while those with $10^{9.5} < L_{18} < 10^{10}\,h^{-2}\,\mathrm{L}_\odot$ are

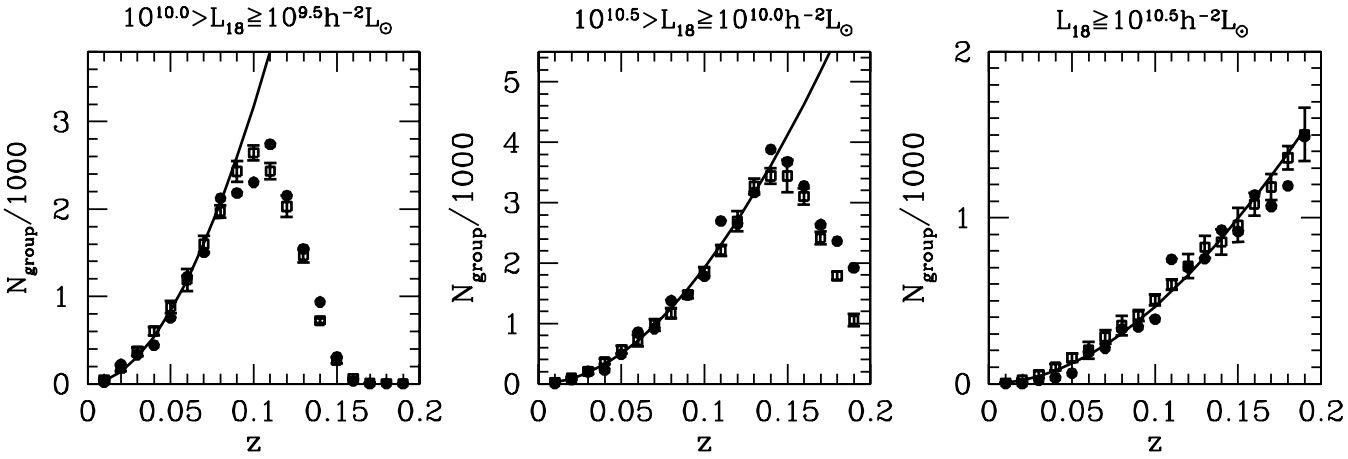

Figure 1. The redshift distributions of galaxy groups for three different bins in L_{18} (as indicated). Open squares with errorbars are the mean and 1σ variance of the number counts for groups in eight independent MGRSs, while solid dots correspond to the number counts of groups in the 2dFGRS. Solid lines indicate the expected value for a constant group number density. As shown in YMBJ, groups with $L_{18} \geqslant 10^{10.5}\,h^{-2}\,\mathrm{L}_\odot$ are complete for $z < 0.2$.

Table 1. The 2dFGRS group correlation functions.

Sample	N	$z_{\max}$	d h^{-1} Mpc	$s_0(\gamma = 1.8)$ h^{-1} Mpc	$r_0(\gamma = 1.8)$ h^{-1} Mpc	r_0 h^{-1} Mpc	γ	$b/b(O6)$	β
(1)	(2)	(3)	(4)	(5)	(6)	(7)	(8)	(9)	(10)
O1	250	0.20	43.77	19.30 ± 1.73	–	–	–	–	–
O2	500	0.20	34.74	16.09 ± 1.42	15.05 ± 0.83	15.44	2.38	1.79 ± 0.11	0.22 ± 0.27
O3	1000	0.20	27.57	14.84 ± 0.63	12.79 ± 0.58	13.53	2.16	1.58 ± 0.07	0.17 ± 0.16
O4	2000	0.20	21.88	12.68 ± 0.41	11.83 ± 0.48	11.82	1.79	1.34 ± 0.04	0.28 ± 0.15
O5	4000	0.20	17.37	10.84 ± 0.32	9.62 ± 0.32	9.36	1.72	1.19 ± 0.03	0.36 ± 0.07
O6	8000	0.20	13.79	9.26 ± 0.22	8.11 ± 0.17	8.02	1.77	1.00	0.35 ± 0.08
O7	16 000	0.20	10.94	8.12 ± 0.17	6.94 ± 0.23	6.54	1.68	0.87 ± 0.02	0.48 ± 0.07
O8	16 000	0.13	7.22	6.24 ± 0.20	4.77 ± 0.12	4.78	1.86	0.63 ± 0.03	0.50 ± 0.12
O9	8000	0.08	5.67	4.55 ± 0.40	3.55 ± 0.23	3.70	1.85	0.48 ± 0.05	0.68 ± 0.26

complete down to $z \sim 0.08$ (left-hand panel). Note that the redshift distributions of the MGRS agree nicely with the 2dFGRS, indicating that we have properly accounted for the various incompleteness effects when constructing our mock surveys (see van den Bosch et al. 2004a; Yang et al. 2004a for details). With these considerations, we can construct volume-limited group samples by ranking all groups according to their L_{18}. The brightest N groups then form a volume-limited subsample. Using this ranking-technique we construct nine subsamples, Oi, where $i = 1, 2, \ldots, 9$ correspond to different choices of N and the maximum redshift $z_{\max}$. Rather than characterizing different subsamples by N and $z_{\max}$, we use the mean group separation, $d = n^{-1/3}$, where n is the number density of groups in the subsample. Table 1 lists the subsamples thus selected, and which form the observational data base for our analyses.

In YMBJ, we also applied our group finder to eight MGRSs constructed using exactly the same selection criteria as the 2dFGRS (see Yang et al. 2004a for details). Note that in the present MGRSs, we also include fibre collisions in the way described in van den Bosch et al. (2004b). Here we make use of these mock group catalogues to test the relation between the groups and the dark matter haloes. For this purpose, we generate eight dark halo catalogues from the eight MGRSs. In which, we select *all* the dark matter haloes in our 'virtual universe' with $0.01 < z < 0.20$ that are within the area of the sky covered by 2dFGRS, where the completeness is larger than 0.8. Note that these haloes are *not* exactly the same as those corresponding to all selected groups, because the later are not complete due to the survey selection effect. Subsamples of mock groups and dark matter haloes are constructed in the same way as the 2dF group samples, i.e. according to the L_{18} ranking for mock groups or according to halo mass ranking for dark matter haloes. We denote these two sets of subsamples as Mi (for mock groups) and Hi (for dark matter haloes). Subsamples Oi, Mi and Hi all have the same number of objects for a given i. As we have eight independent MGRSs, for each i we have eight independent mock subsamples and eight halo subsamples. All errorbars quoted below are based on the scatter among these subsamples.

Column 1 indicates the sample ID. Columns 2 (number of groups) and 3 (redshift range: $0.01 \leqslant z \leqslant z_{\max}$) indicate the selection criteria. Column 4 lists the mean separation ($d = n^{-1/3}$) of the selected groups. Columns 5 and 6 list the redshift space and real-space correlation lengths, respectively, obtained fitting $\xi(s)$ with $\xi(s) = (s/s_0)^{1.8}$ ($5 \leqslant s \leqslant 15\ h^{-1}$ Mpc) and $w_{\rm p}(r_{\rm p})$ using $\xi(r) = (r/r_0)^{1.8}$ ($3 \leqslant r_{\rm p} \leqslant 15\ h^{-1}$ Mpc), columns 7 and 8 indicate the r_0 and γ obtained fitting $w_{\rm p}(r_{\rm p})$ using $\xi(r) = (r/r_0)^{\gamma}$. Column 9 indicates the bias of groups relative to that of the fiducial O6 sample, and column 10, finally, lists the β parameter. All the error bars listed in this table are 1σ variances obtained from the scatter among eight mock group samples.

3 THE TWO-POINT CORRELATION FUNCTION

We compute the group–group (or halo–halo) 2PCF $\xi(r_\mathrm{p}, \pi)$ using the following estimator

$$\xi(r_\mathrm{p}, \pi) = \frac{\langle RR\rangle\langle DD\rangle}{\langle DR\rangle^2} - 1 \tag{1}$$

with $\langle DD\rangle$, $\langle RR\rangle$ and $\langle DR\rangle$ the number of group–group, random–random and group–random pairs with separation (r_p, π) (Hamilton 1993). Here r_p and π are, respectively, the pair separations perpendicular and parallel to the line of sight. Explicitly, for a pair $(\boldsymbol{s_1}, \boldsymbol{s_2})$, with $\boldsymbol{s}_i = cz_i\hat{\boldsymbol{r}}_i/H_0$, we define

$$\pi = \frac{\boldsymbol{s}\cdot\boldsymbol{l}}{|\boldsymbol{l}|}, \qquad r_\mathrm{p} = \sqrt{\boldsymbol{s}\cdot\boldsymbol{s} - \pi^2}, \tag{2}$$

where $\boldsymbol{l} = (1/2)(\boldsymbol{s}_1 + \boldsymbol{s}_2)$ is the line of sight intersecting the pair, and $\boldsymbol{s} = \boldsymbol{s}_1 - \boldsymbol{s}_2$.

Except for O1, all the 2dF samples listed in Table 1 contain sufficient numbers of galaxy groups for a proper determination of the 2PCF. Fig. 2 shows the contour-plots for the $\xi(r_\mathrm{p}, \pi)$ of some of these samples. Panels from the upper left- to the upper right-hand side and from lower left- to lower right-hand side correspond to samples O3 – O8. Note that these $\xi(r_\mathrm{p}, \pi)$ look very different from those of galaxies (e.g. Hawkins et al. 2003): the only deviation from isotropy is a flattening of the contours at large separations due to the infall motion induced by the gravitational action of large-scale structure. Unlike for galaxies, no finger-of-God effect on small scales is present, due to the fact that groups themselves are virialized objects rather than test particles in larger virialized potentials. As we will see in Section 5, this absence of virial motions on small scales makes the interpretation of the redshift distortion easier.

As the redshift-space distortion only affects π, the projection of $\xi(r_\mathrm{p}, \pi)$ along the π-axis can remove the infall induced distortions and give a function that is more closely related to the real-space correlation function. This projected 2PCF, $w_\mathrm{p}(r_\mathrm{p})$, is related to the real-space 2PCF, $\xi(r)$, through a simple Abel transform

$$w_\mathrm{p}(r_\mathrm{p}) = \int_{-\infty}^{\infty} \xi(r_\mathrm{p}, \pi)\,\mathrm{d}\pi = 2\int_{r_\mathrm{p}}^{\infty} \xi(r)\,\frac{r\,\mathrm{d}r}{\sqrt{r^2 - r_\mathrm{p}^2}} \tag{3}$$

(Davis & Peebles 1983). Therefore, if the real-space 2PCF is a power-law, $\xi(r) = (r_0/r)^\gamma$, the projected 2PCF can be written as

$$w_\mathrm{p}(r_\mathrm{p}) = \sqrt{\pi}\frac{\Gamma(\gamma/2 - 1/2)}{\Gamma(\gamma/2)}\left(\frac{r_0}{r_\mathrm{p}}\right)^\gamma r_\mathrm{p}. \tag{4}$$

The black dots in the upper panels of Fig. 3 show the projected correlation function $w_\mathrm{p}(r_\mathrm{p})$ of 2dFGRS groups estimated from $\xi(r_\mathrm{p}, \pi)$ using equation (3) with the integration range set to $|\pi| \leqslant 40\ h^{-1}$ Mpc. For comparison, we also plot $w_\mathrm{p}(r_\mathrm{p})$ for the mock groups (solid line with errorbars). The three panels correspond to samples with mean separation $d = 34.74$, 17.37 and $7.22\,h^{-1}$ Mpc, as indicated. Overall, the agreement between data and mock

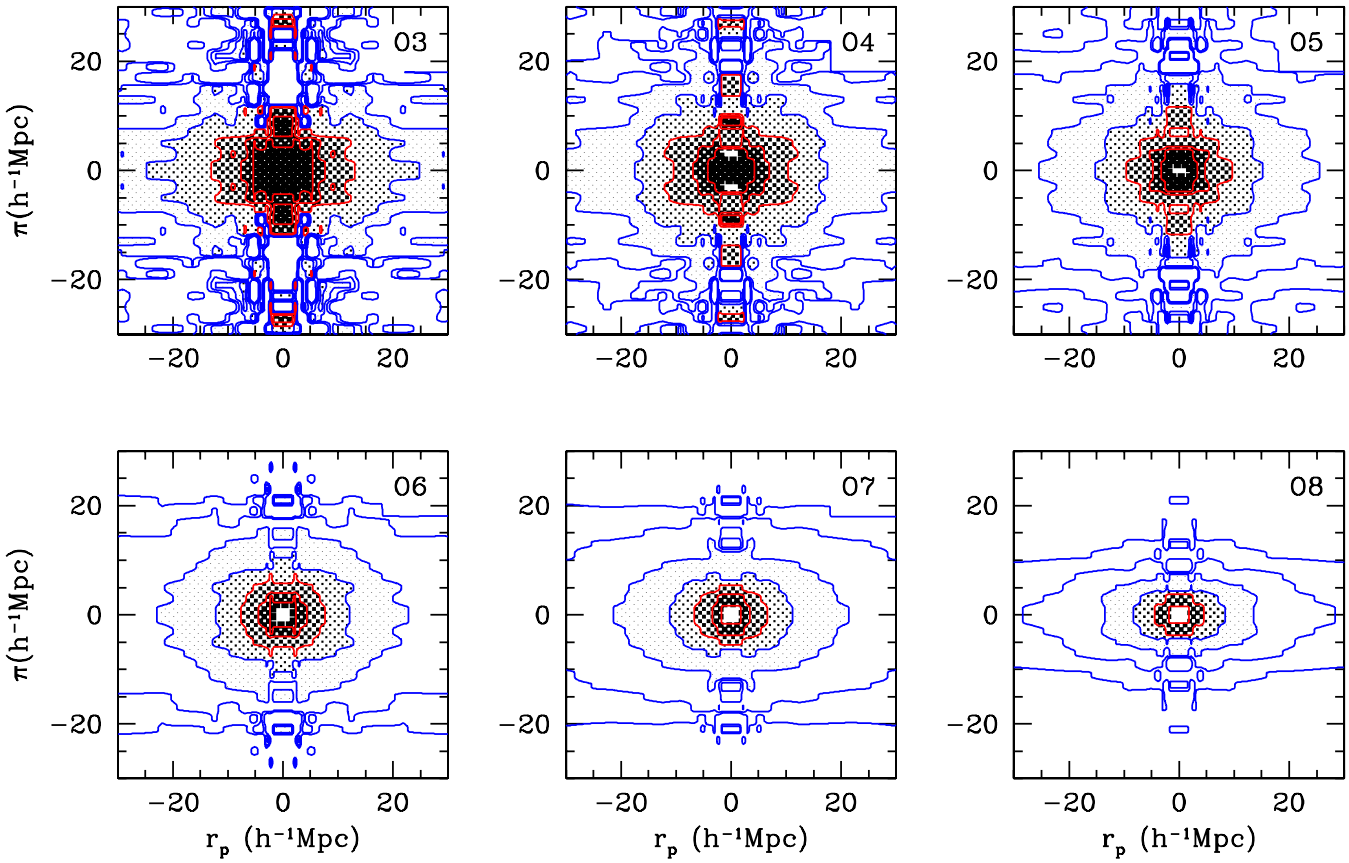

Figure 2. The two-point correlation function, $\xi(r_\mathrm{p}, \pi)$, for various group samples (as indicated) extracted from the 2dFGRS. From the upper left- to the upper right-hand side, then the lower left- to the lower right-hand side, the samples have smaller mean intergroup separations d (see Table 1), indicating an increased inclusion of less massive systems. Note that samples with smaller d reveal a more pronounced flattening of the contours (see also Section 5 and the right-hand panel of Fig. 7).

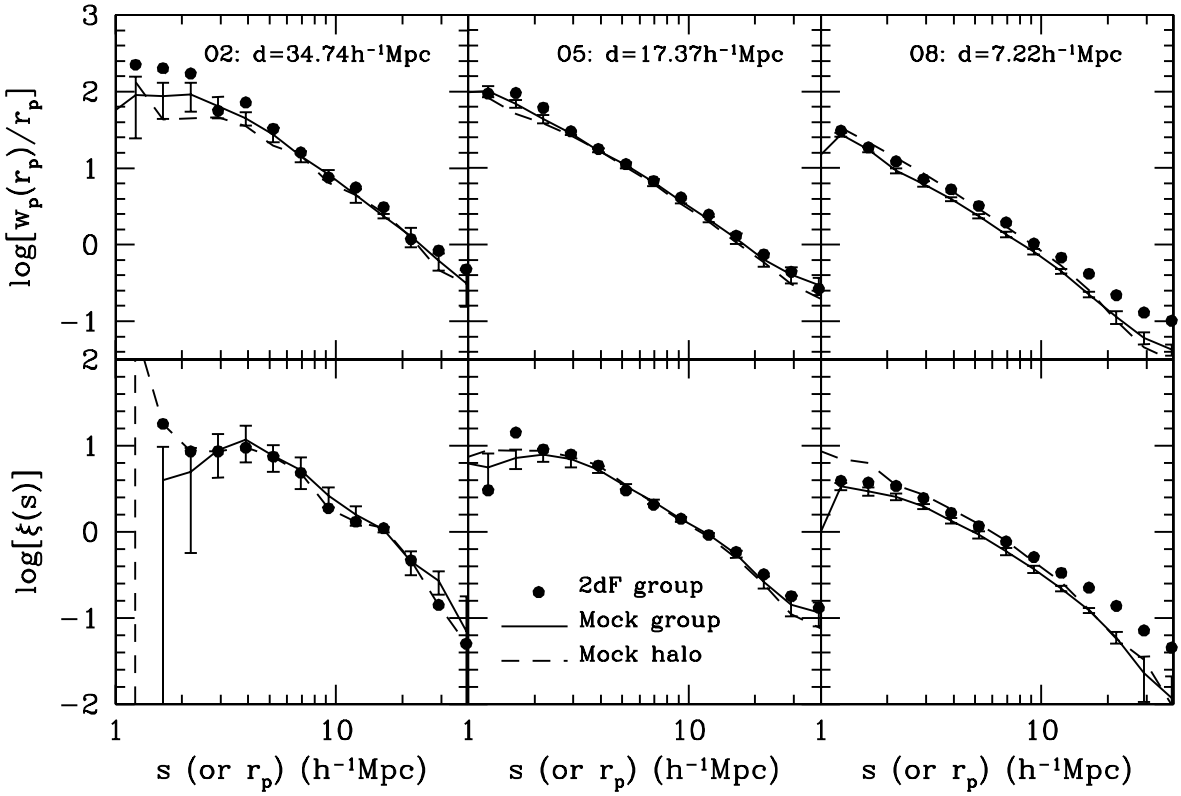

Figure 3. The projected correlation function, $w_p(r_p)$ (upper panels), and redshift space correlation function, $\xi(s)$ (lower panels), of groups and dark matter haloes. Solid dots correspond to the groups extracted from the 2dFGRS, while solid and dashed lines indicate the same results, but obtained for the samples of mock galaxies and their corresponding dark matter haloes, respectively. The errorbars associated with the solid lines indicate the 1σ variance obtained from the eight independent MGRSs. Results are shown for three different values of the mean group separation, d, as indicated.

is extremely good. An exception is the large scales in sample O8 ($d = 7.22\ h^{-1}$ Mpc),[1] where the $w_p(r_p)$ of the mock groups is significantly underestimated. This is due to the fact that this sample occupies a small, nearby volume, which in our MGRSs is represented by a small box-size simulation that does not properly sample the large(r) scale structure (see Yang et al. 2004a for details).

In most previous studies of group–group correlation functions, the redshift-space 2PCF $\xi(s)$, rather than the real-space 2PCF, was used to represent the clustering strength (Croft et al. 1997; Park & Lee 1998; Bahcall et al. 2003; Zandivarez et al. 2003; Padilla et al. 2004). In order to allow for a comparison we also compute the redshift-space correlation functions, which are shown in the lower panels of Fig. 3. Here again, the results for the mock samples match those of the 2dFGRS samples remarkably well, except at large radii in sample O8.

4 THE RELATION BETWEEN GALAXY GROUPS AND DARK MATTER HALOES

So far we have focused on the 2PCFs for groups in the 2dFGRS and in our MGRSs. We now examine whether or not these results can be understood in terms of 2PCFs between dark matter haloes in the ΛCDM concordance cosmology. As the clustering properties of CDM haloes are well understood (Mo & White 1996, 2002; Jing 1998; Sheth & Tormen 1999; Jenkins et al. 2001; Sheth, Mo & Tormen 2001; Seljak & Warren 2004), such a connection between the populations of galaxy groups and dark matter haloes enables us to understand the clustering of groups in a cosmological context.

As mentioned above, the luminosity of a group, L_{18}, is tightly correlated to the mass of its host halo. Therefore, groups ranked by the value of L_{18} may be used to represent dark matter haloes ranked by halo mass. To check this, we compare the correlation functions of mock group samples (M1, M2, etc.) with those of dark matter halo samples (H1, H2, etc.). The results are shown as solid and dashed lines, respectively, in Fig. 3. Note that the correlation function of mass-ranked dark matter haloes matches that of L_{18}-ranked groups remarkably well.

In order to facilitate a more qualitative comparison, we fit $w_p(r_p)$ with a single power law of the form (4) over the range $3 < r_p < 15\ h^{-1}$ Mpc. The goodness of fit is based on a simple χ^2 criterion, where the errors used for each data point are obtained from the scatter among eight independent mock samples [the errors due to cosmic variance are typically larger than the statistical errors on each individual $w_p(r_p)$ measurement]. Over the r_p range considered here, a power law is an acceptable model. We treat the slope γ either as a free parameter or keep it fixed at a value of $\gamma = 1.8$. In the latter case, the fit is used to determine only the correlation length r_0. The differences in the correlation lengths estimated with fixed or free γ is less than 10 per cent. Fig. 4 shows r_0 (obtained keeping γ fixed) as a function of mean group separation for both mock groups and dark matter haloes. The agreement between the

[1] We find a similar discrepancy between data and model for sample O9, which is limited to an even smaller volume, with an even smaller mean separation, than sample O8.

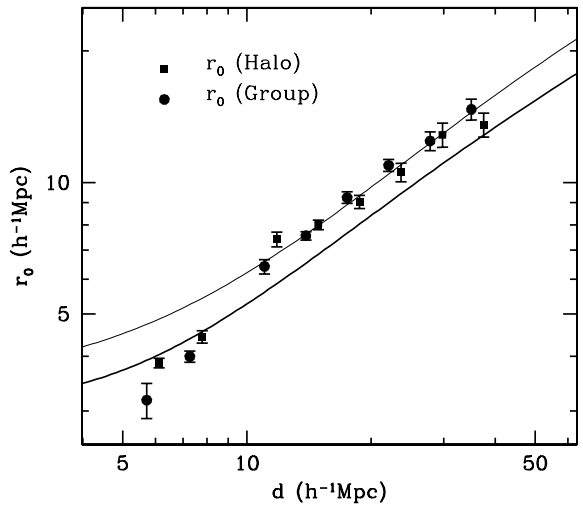

Figure 4. The relation between the correlation length, r_0, and the mean intergroup separation, d, for groups (solid circles) and dark matter haloes (solid squares) in the MGRSs (errorbars indicate the 1σ scatter among the eight independent mock catalogues). For clarity, the results for the dark matter haloes have been shifted to the right by $\Delta \log d = 0.03$. Note the good agreement between groups and haloes, indicating that groups ranked by luminosity can be compared directly to dark matter haloes ranked by halo mass. Thick and thin solid lines correspond to theoretical predictions based on the halo bias models of SW04 and SMT01, respectively. Note that the difference between these two model predictions is larger than the scatter among our eight MGRSs (see Section 6 for a detailed discussion).

groups and dark matter haloes is remarkably good, especially for massive/bright systems (note that they have been offset from each other by $\Delta \log d = 0.03$ for clarity). At small values of d, i.e. for faint groups and low-mass haloes, the groups have slightly lower correlation lengths than the dark matter haloes. This discrepancy is at least partly due to the incompleteness of the 2dFGRS (which we have mimicked in our MGRSs). As a result of this incompleteness, which is not present for the dark matter haloes, the true mean intergroup separation is overestimated. This effect is less important for larger groups; although some of the member galaxies are missed, they still contain sufficient members to be identified as a group.

We have also estimated the redshift-space correlation lengths, s_0. In this case, we adopt a simple power-law model, $\xi(s) = (s/s_0)^{1.8}$, to fit $\xi(s)$ over the range $5 < s < 15\ h^{-1}$ Mpc. The lower limit of s adopted here is larger than that of r_p used in fitting $w_p(r_p)$, because the redshift-space correlation is not well described by a power law at smaller separations (see lower panels of Fig. 3). As for the real-space correlation lengths, we find extremely good agreement between the s_0 of mock groups and dark matter haloes (not shown).

All these results provide strong support for a tied correlation between group luminosity and halo mass, clearly demonstrating that the groups ranked by luminosity can be compared meaningfully to dark matter haloes ranked by halo mass.

5 ABUNDANCE DEPENDENCE OF GROUP CORRELATION FUNCTION

Having established a tied correlation between group luminosity and halo mass, we now return to our 2dFGRS group catalogue. Using the same fitting procedure as described above, we determine the correlation lengths r_0 and s_0 as well as the slope γ for 2dFGRS groups. Results are listed in Table 1 (columns 5–8). In Fig. 5 we plot the correlation lengths r_0 (left-hand panel) and s_0 (right-hand panel) as a function of d, obtained assuming a fixed slope of $\gamma = 1.8$. For comparison, the right-hand panel also shows the SDSS results (open squares) obtained by Bahcall et al. (2003) and the 2dFGRS percolation-inferred galaxy group (2PIGG) results (open circles) obtained by Padilla et al. (2004) from the 2dFGRS. All three measurements are in excellent agreement with each other. Fitting our r_0–d and s_0–d relations by power laws, we obtain $r_0 = 1.11\ d^{0.75}$ and $s_0 = 1.88\ d^{0.61}$. These power laws are shown as dot-dashed lines in Fig. 5.

The correlation strength of a sample can also be described by the ratio of its projected correlation function and that of a fiducial sample. Fig. 6 plots the ratio $w_p(r_p)/w_{p,O6}(r_p)$ as a function of r_p, where O6 has been used as the fiducial sample. Note that $w_p(r_p)/w_{p,O6}(r_p)$ is roughly constant with r_p, indicating that the slope of the

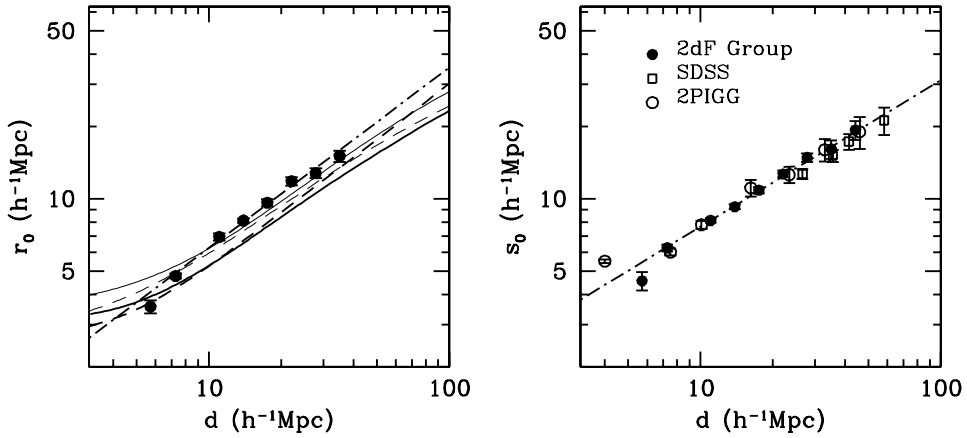

Figure 5. Left-hand panel, the relation between r_0 and d for groups selected from the 2dFGRS (solid dots). Errorbars indicate the 1σ variance from eight independent mock group samples. The solid and dashed lines are model predictions for a ΛCDM cosmology with $\sigma_8 = 0.9$ and 0.7, respectively. Thick and thin lines are based on the bias models of SW04 and SMT01, respectively. The dot-dashed line, finally, corresponds to the best-fitting power-law relation, $r_0 = 1.11\ d^{0.75}$. Right-hand panel, the relation between the redshift-space correlation length, s_0, and mean group separation, d, for our 2dFGRS group catalogue (solid dots), compared with those of the SDSS (Bahcall et al. 2003) and 2PIGG (Padilla et al. 2004). The dot-dashed line corresponds to the best-fitting power-law, $s_0 = 1.88\ d^{0.61}$.

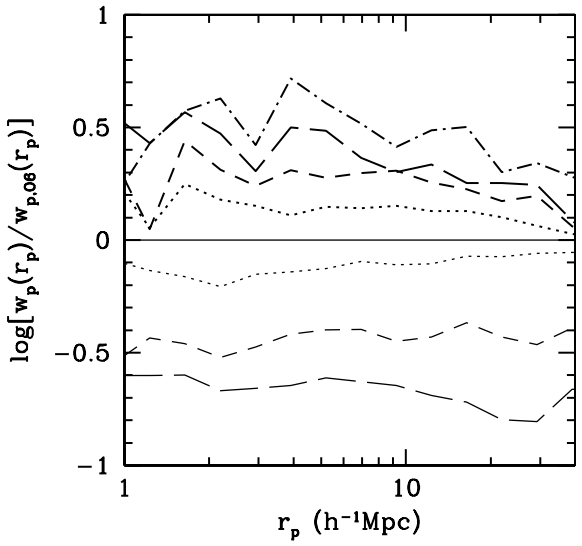

Figure 6. The ratio of the projected 2PCF of various samples of 2dFGRS groups relative to the fiducial sample O6, $w_{\rm p}(r_{\rm p})/w_{\rm p,O6}(r_{\rm p})$. Note that the projected 2PCFs of different samples have very similar slopes but very different amplitudes.

correlation function is roughly the same for different samples. However, the overall *amplitude* of the ratio has a clear trend with d. To illustrate this we define the *relative* bias b/b(O6) as the mean value of the ratio $w_{\rm p}(r_{\rm p})/w_{\rm p,06}(r_{\rm p})$ in the range $5 \leqslant r_{\rm p} \leqslant 10\,h^{-1}$ Mpc, and plot b/b(O6) as a function of mean group separation in the left-hand panel of Fig. 7 (numerical values are listed in column 9 of Table 1).

For a given sample the value of s_0 is systematically larger than r_0 (cf. columns 5 and 6). This is due to the enhancement of clustering in redshift-space due to gravitational infall. To quantify this redshift distortion, we use the model of Kaiser (1987; see also Hamilton 1992). According to linear theory, the infall velocities around density perturbations affect the observed correlation function as

$$\xi_{\rm lin}(r_{\rm p}, \pi) = \xi_0(s)\mathcal{P}_0(\mu) + \xi_2(s)\mathcal{P}_2(\mu) + \xi_4(s)\mathcal{P}_4(\mu), \quad (5)$$

where $\mathcal{P}_l(\mu)$ is the lth Legendre polynomial, and μ is the cosine of the angle between the line of sight and the redshift-space separation $\boldsymbol{s}$. According to linear perturbation theory the angular moments can be written as

$$\xi_0(s) = \left(1 + \frac{2\beta}{3} + \frac{\beta^2}{5}\right)\xi(r), \quad (6)$$

$$\xi_2(s) = \left(\frac{4\beta}{3} + \frac{4\beta^2}{7}\right)[\xi(r) - \overline{\xi}(r)], \quad (7)$$

$$\xi_4(s) = \frac{8\beta^2}{35}\left[\xi(r) + \frac{5}{2}\overline{\xi}(r) - \frac{7}{2}\hat{\xi}(r)\right], \quad (8)$$

with

$$\overline{\xi}(r) = \frac{3}{r^3}\int_0^r \xi(r')r'^2\,{\rm d}r', \quad (9)$$

and

$$\hat{\xi}(r) = \frac{5}{r^5}\int_0^r \xi(r')r'^4\,{\rm d}r'. \quad (10)$$

In the above expressions, β is the linear distortion parameter, which can be written as $\beta = \Omega_m^{0.6}/b$, where b is the bias parameter of the objects under consideration. Given the real-space correlation function $\xi(r) = (r/r_0)^{\gamma}$, which can be obtained from $w_{\rm p}(r_{\rm p})$, equation (5) can be used to model $\xi(r_{\rm p}, \pi)$ on linear scales. By comparing the model predictions with the observed $\xi(r_{\rm p}, \pi)$, one can easily obtain the value of β. We use a simple χ^2 fit of the observed $\xi(r_{\rm p}, \pi)$ in the range $8 \leqslant s \leqslant 20\,h^{-1}$ Mpc to equation (5) to probe the only free parameter β. In the fitting, each data point for $\xi(r_{\rm p}, \pi)$ is weighted by the error based on the scatter among eight independent mock samples. The right-hand panel of Fig. 7 plots the β values thus obtained for both mock groups (squares with errorbars) and 2dFGRS groups (solid dots). Although there is significant scatter, there is a clear trend that groups with a smaller mean separation d (i.e. less luminous groups) have larger β and thus a stronger distorted redshift-space correlation function (this is also directly visible from Fig. 2). The numerical values of β for the 2dFGRS groups are listed

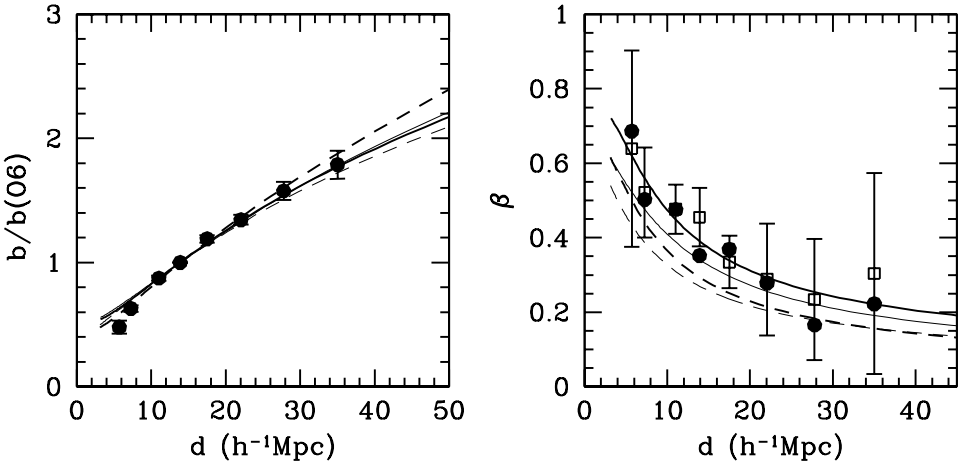

Figure 7. Left-hand panel, the relative bias, b/b(O6), of groups as a function of mean group separation d. These relative biases are computed from the relation in Fig. 6 using the radial interval with $5 \leqslant r_{\rm p} \leqslant 10\,h^{-1}$ Mpc. Note that more massive systems (i.e. with larger d) are more strongly biased. Right-hand panel, the redshift distortion parameter β of mock (open squares with errorbars) and 2dFGRS groups (solid dots) as a function of d. In both panels, the various lines correspond to the model predictions, with the same line styles as in Fig. 5. Errorbars in both panels indicate the 1σ variance from eight independent mock group samples.

in column 10 of Table 1, together with the 1σ variances obtained from the scatter among the eight MGRSs.

6 COMPARISON WITH THEORETICAL PREDICTIONS

The tests described in the previous sections show that the abundance dependence of the group–group correlation function can be explained in terms of the halo–halo correlation function (after all, we constructed our group finder to associate galaxies according to their common dark matter halo). This suggests that we may compare the 2dFGRS group–group 2PCF with halo–halo correlation functions predicted by current models of structure formation in order to constrain cosmological parameters.

The mean number density of dark matter haloes with mass $M > M_1$ can be estimated through,

$$\overline{n}(M > M_1) = \int_{M_1}^{\infty} n(M)\,\mathrm{d}M, \tag{11}$$

where $n(M)$ is the mass function of dark matter haloes, which can be estimated analytically from the Press–Schechter formalism (e.g. Press & Schechter 1974; Sheth et al. 2001, hereafter SMT01). The mean bias for haloes with mass exceeding M_1 can be estimated from

$$\overline{b}(M > M_1) = \frac{1}{\overline{n}(M > M_1)} \int_{M_1}^{\infty} n(M)\,b(M)\,\mathrm{d}M, \tag{12}$$

where $b(M)$ is the bias parameter of dark matter haloes (Mo & White 1996; Jing 1998; Sheth & Tormen 1999; SMT01; Seljak & Warren 2004, hereafter SW04). Throughout we use the halo mass function of SMT01, which has been shown to be in excellent agreement with numerical simulations (e.g. Jenkins et al. 2001; White 2002). For the halo bias parameter, we use the models of both SMT01 and SW04 for comparison.

Using $d = n^{-1/3}$ and $r_0 = b^{2/1.8}\, r_{0,\mathrm{DM}}$, where $r_{0,\mathrm{DM}}$ is the correlation length of the dark matter, we compute $r_0(d)$. Here the linear power spectrum is computed using the transfer function of Eisenstein & Hu (1998), which properly accounts for the baryons, while the non-linear power spectrum, which is required in calculating the dark matter correlation function and $r_{0,\mathrm{DM}}$, is computed using the fitting formula of Smith et al. (2003). The solid lines in Fig. 4 show the model predictions thus obtained using the bias models of SW04 (thick line) and of SMT01 (thin line). The difference between the two bias models is quite large, and much larger than the 1σ variance among our 8 MGRSs. Thus, although the r_0–d relation can now be accurately determined from observational data the current models for halo bias are not yet accurate enough to allow one to obtain stringent constraints on model parameters (see below).

In the left-hand panel of Fig. 5 we compare the results obtained for the 2dFGRS groups with various theoretical predictions. The thin solid line corresponds to a standard ΛCDM model with $\sigma_8 = 0.9$, obtained using the bias model of SMT01. The thin dashed line indicates the prediction for the same bias model, but with $\sigma_8 = 0.7$. Based on this, one might conclude that the observational data are in better agreement with $\sigma_8 = 0.9$. However, if we use the bias model of SW04 (thick solid and dashed lines), the $\sigma_8 = 0.7$ cosmology matches the data better. Note that although the bias model of SW04 may be more accurate than earlier models, the uncertainty of the bias parameter at the massive end is still 10 to 20 per cent, which is much larger than the error on the observational results. Clearly, the halo bias model has to be improved further, in order to make full use of the constraining power of the present observational results.

Fig. 7 compares the theoretical predictions for the *relative* bias $b/b(\mathrm{O6})$ (left-hand panel) and the redshift-distortion parameter $\beta = \Omega_m^{0.6}/b$ (right-hand panel, assuming $\Omega_m = 0.3$) with our observational results from the 2dFGRS. As a result of the normalization at a given d, the predicted relation between the relative bias and d is quite similar for different models (i.e. the relative bias is fairly insensitive to the value of σ_8). More importantly, all model predictions are in good agreement with the observational data. The observed value of β as a function of d is also well described by the theory, but the errorbars are too big to provide stringent constraint on model parameters.

7 UNDERSTANDING THE SHAPE OF THE CORRELATION FUNCTION OF GALAXIES

It is well known that the real-space correlation function of (normal) galaxies is remarkably well described by a single power law for $r \lesssim 10\,h^{-1}$ Mpc. Given that the *mass* correlation function predicted for typical ΛCDM cosmologies is significantly curved on these scales, it is important to understand the origin of this power-law behaviour. Jing, Mo & Börner (1998) were the first to show that, if the number of galaxies in a dark matter halo increases with halo mass as a power law, with a power index moderately below unity, and if the number density distribution of galaxies in massive haloes has approximately the same profile as the dark matter, the observed power-law shape of the galaxy correlation function can be reproduced. This kind of galaxy bias on small scales is now well understood in the current halo occupation model (Peacock & Smith 2000; Seljak 2000; Scoccimarro et al. 2001; Berlind & Weinberg 2002; Bullock, Wechsler & Somerville 2002; Jing, Börner & Suto 2002; Scranton 2002; Berlind et al. 2003; van den Bosch et al. 2003; Yang, Mo & van den Bosch 2003). In the halo model, the 2PCF of galaxies can be decomposed into two terms:

$$\xi(r) = \xi_{1\mathrm{h}}(r) + \xi_{2\mathrm{h}}(r), \tag{13}$$

where $\xi_{1\mathrm{h}}$ represents the correlation due to pairs of galaxies within the same halo (the 'one-halo' term), and $\xi_{2\mathrm{h}}$ describes the correlation due to galaxies that occupy different haloes (the 'two-halo' term). In the standard ΛCDM model $\xi(r)$ has a characteristic scale at $r \sim 1$–$2\,h^{-1}$ Mpc, where the dominating contribution to the 2PCF makes a transition from the one- to the two-halo term. Therefore, some departure from a pure power law is expected for populations of galaxies for which the one- and two-halo terms are not well balanced. In fact, such a departure, albeit small, has recently been found in the projected correlation function of SDSS galaxies (Zehavi et al. 2004).

The various analyses in the previous sections have shown that our groups selected from the 2dFGRS are nicely related to dark matter haloes. Therefore, we can directly measure the 'one-' and 'two-halo' terms of the 2PCF, by simply determining whether both galaxies of a pair reside in the same group (this pair adds to the one-group term), or whether they reside in two different groups (in which case the pair adds to the two-group term). Fig. 8 plots the projected two-point correlation functions of 2dFGRS galaxies that are associated with groups of different abundances. In addition to $w_{\mathrm{p,tot}}(r_{\mathrm{p}})$, we also indicate the 'one-halo' (one-group) and 'two-halo' (two-group) terms as dot-dashed and dashed lines, respectively. Each galaxy pair is weighted by $\mathcal{W}_{\mathrm{g}} = 1/(c_i c_j)$, where c_i is the survey completeness at the position of galaxy i. On scales $r_{\mathrm{p}} \gtrsim 3\,h^{-1}$ Mpc the projected correlation function $w_{\mathrm{p,tot}}(r_{\mathrm{p}})$ is dominated by the 'two-halo' term, while on smaller scales ($r_{\mathrm{p}} \lesssim 1\,h^{-1}$ Mpc) the 'one-halo' term dominates. Note also that for galaxies residing in massive systems

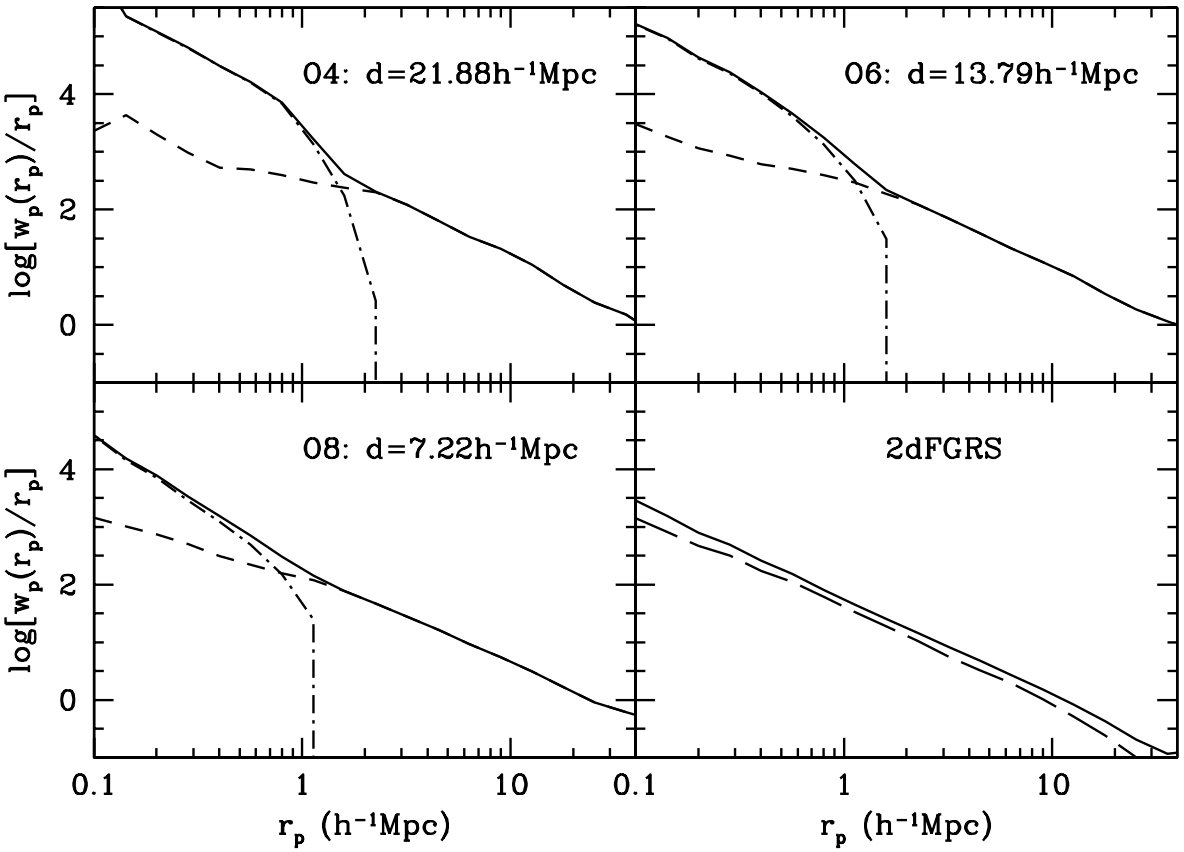

Figure 8. The projected two-point correlation function $w_{\rm p}(r_{\rm p})$ of galaxies in different samples of groups. The solid lines indicate the total correlation functions, $w_{\rm p,tot}(r_{\rm p})$, of all galaxies in group samples O4 (upper left-hand side), O6 (upper right-hand side), O8 (lower left-hand side) and of all (151 820) galaxies in the 2dFGRS sample with $0.01 < z < 0.20$ and completeness >0.8 (lower right-hand side). The dot-dashed and short-dashed lines indicate the corresponding 'one-halo' terms, $w_{\rm p,1h}(r_{\rm p})$, and 'two-halo' terms, $w_{\rm p,2h}(r_{\rm p})$, respectively. Finally, the long-dashed line in the lower right-hand panel indicates the projected correlation function of that half of all galaxies that is not associated with the luminous groups. See the text for details and discussion.

(i.e. large d), the projected correlation function clearly deviates from a pure power-law; for these galaxies, the 'one-halo' term is significantly enhanced. This occurs because the 'one-halo' term contribution from a large group is proportional to $N_{\rm g}(N_{\rm g}-1)$ (where $N_{\rm g}$ is the number of galaxies in the group), while the 'two-halo' term contribution is proportional to b^2, which increases with halo mass at a slower rate. When adding more galaxies to the sample hosted by smaller haloes (i.e. decreasing d), $w_{\rm p,tot}(r_{\rm p})$ becomes better described by a pure power-law. In particular, as shown by the solid line in the lower right-hand panel, when all galaxies (151 820 galaxies with $0.01 < z < 0.20$ and completeness >0.8) are included, the correlation function is well represented by a single power law.

As an additional test, we estimate $w_{\rm p,tot}(r_{\rm p})$ for a sample in which we remove all the galaxies in the most luminous groups such that the total number of galaxies in the sample is halved. Thus, this sample contains only galaxies in low-mass haloes. The correlation function for this sample is shown as the long-dashed line in the lower right-hand panel of Fig. 8. As for the complete sample, the projected correlation function of this sample is well described by a power law, with a slightly shallower slope as for the complete sample.

Therefore, we conclude that the 2PCF of 2dF galaxies reveals a power-law form as long as sufficiently many small mass groups (haloes) are included. For galaxies hosted by massive haloes, however, the 2PCF can deviate significantly from a pure power law.

8 CONCLUSIONS

We have measured the 2PCFs for galaxy groups in the 2dFGRS group catalogue constructed by YMBJ using a halo-based group finder. We have shown that the current data allows one to estimate the correlation function accurately for a wide range of different systems, ranging from isolated galaxies to rich clusters of galaxies. Ranking groups according to their luminosities, L_{18}, we have studied how the correlation of groups depends on group abundance. Consistent with previous studies (e.g. Bahcall et al. 2003; Padilla et al. 2004), we found that the amplitude of the correlation function increases with group luminosity (richness). The dependence of the redshift-space correlation length s_0 on the mean intergroup separation d can be quantified as $s_0 = 1.88\, d^{0.61}$, while the real-space correlation length r_0 reveals a somewhat steeper dependence: $r_0 = 1.11\, d^{0.75}$.

Using mock group catalogues, obtained from detailed mock galaxy redshift surveys, and the corresponding catalogues of dark matter haloes, we have shown that the correlation functions of the 2dFGRS groups can be understood in terms of halo–halo clustering. The observed correlation length (and the corresponding bias factor) as a function of group abundance is well reproduced by associating galaxy groups with dark matter haloes in the standard ΛCDM model. In particular, the groups ranked by L_{18} match extremely well with dark matter haloes ranked by mass. We found, however, that current theoretical predictions for the halo–halo correlation functions are not yet accurate enough to allow us to use the observational

results to put stringent constraints on model parameters in the ΛCDM cosmogony.

Analysing the correlation function for galaxies associated with different groups, we were able to bisect the 2PCF of galaxies in terms of a group–group correlation function and a term due to galaxies in the same group. As our groups are closely related to dark matter haloes, this split corresponds to the one- and two-halo terms of the correlation function. We have shown how the power-law form of the (projected) correlation function is broken when only considering galaxies in massive haloes, and how the balance between the 'one-' and 'two-halo' terms changes with halo mass.

ACKNOWLEDGMENT

Numerical simulations used in this paper were carried out at the Astronomical Data Analysis Centre (ADAC) of the National Astronomical Observatory, Japan. We thank the 2dF team for making their data publicly available.

REFERENCES

Bahcall N. A., 1988, ARA&A, 26, 631
Bahcall N. A., West M. J., 1992, ApJ, 392, 419
Bahcall N. A., Dong F, Hao L., Bode P., Annis J., Gunn J. E., Schneider D. P., 2003, ApJ, 599, 814
Berlind A. A., Weinberg D. H., 2002, ApJ, 575, 587
Berlind A. A. et al., 2003, ApJ, 593, 1
Bullock J. S., Wechsler R. H., Somerville R. S., 2002, MNRAS, 329, 246
Colless M. et al., 2001, MNRAS, 328, 1039
Croft R. A. C., Dalton G. B., Efstathiou G., Sutherland W. J., Maddox S. J., 1997, MNRAS, 291, 305
Davis M., Peebles P. J. E., 1983, ApJ, 267, 465
Eisenstein D. J., Hu W., 1998, ApJ, 496, 605
Eke V. R. et al., 2004, MNRAS, 348, 866
Hamilton A. J. S., 1992, ApJ, 385, L5
Hamilton A. J. S., 1993, ApJ, 417, 19
Hawkins E. et al., 2003, MNRAS, 346, 78
Jenkins A., Frenk C. S., White S. D. M., Colberg J. M. Cole S., Evrard A. E., Couchman H. M. P., Yoshida N., 2001, MNRAS, 321, 372
Jing Y. P., 1998, ApJ, 503, L9
Jing Y. P., Mo H. J., Börner G., 1998, ApJ, 494, 1
Jing Y. P., Börner G., Suto Y., 2002, ApJ, 564, 15
Kaiser N., 1984, ApJ, 284, L9
Kaiser N., 1987, MNRAS, 227, 1
Kepner J., Fan X., Bahcall N., Gunn J., Lupton R., Xu G., 1999, ApJ, 517, 78
Kim R. J. S. et al., 2002, AJ, 123, 20
Kochanek C. S., White M., Huchra J., Macri L., Jarrett T. H., Schneider S. E., Mader J., 2003, ApJ, 585, 161
Mo H. J., White S. D. M., 1996, MNRAS, 282, 347
Mo H. J., White S. D. M., 2002, MNRAS, 336, 112
Mo H. J., Jing Y. P., White S. D. M., 1996, MNRAS, 282, 1096
Navarro J. F., Frenk C. S., White S. D. M., 1997, ApJ, 490, 493
Padilla N. D. et al., 2004, MNRAS, 352, 211
Park C., Lee S., 1998, J. Korean Astron. Soc., 31, 105
Peacock J. A., Smith R. E., 2000, MNRAS, 318, 1144
Postman M., Lubin L. M., Gunn J. E., Oke J. B., Hoessel J. G., Schneider D. P., Christensen J. A., 1996, AJ, 111, 615
Press W. H., Schechter P., 1974, ApJ, 187, 425
Scoccimarro R., Sheth R. K., Hui L., Jain B., 2001, ApJ, 546, 20
Scranton R., 2002, MNRAS, 332, 697
Seljak U., 2000, MNRAS, 318, 203
Seljak U., Warren M. S., 2004, MNRAS, 355, 129 (SW04)
Sheth R. K., Tormen G., 1999, MNRAS, 308, 119
Sheth R. K., Mo H. J., Tormen G., 2001, MNRAS, 323, 1 (SMT01)
Smith R. E. et al., 2003, MNRAS, 341, 1311
van den Bosch F. C., Yang X., Mo H. J., 2003, MNRAS, 340, 771
van den Bosch F. C., Norberg P., Mo H. J., Yang X., 2004a, MNRAS, 352, 1302
van den Bosch F. C., Yang X., Mo H. J., Norberg P., 2004b, MNRAS, in press (astro-ph/0406246)
White M., 2002, ApJS, 143, 241
White M., Kochanek C. S., 2002, ApJ, 574, 24
Yang X., Mo H. J., van den Bosch F. C., 2003, MNRAS, 339, 1057
Yang X., Mo H. J., Jing Y. P., van den Bosch F. C., Chu Y. Q., 2004a, MNRAS, 350, 1153
Yang X., Mo H. J., van den Bosch F. C., Jing Y. P., 2004b, preprint (astro-ph/0405234) (YMBJ)
Zandivarez A., Merchan M. E., Padilla N. D., 2003, MNRAS, 344, 247
Zehavi I. et al., 2004, ApJ, 608, 16

APPENDIX: THE HALO-BASED GROUP FINDER AND THE ASSIGNMENT OF L_{18}

A1 The group finder

In a recent paper, Yang et al. (2004b) developed a halo-based group finder that can successfully assign galaxies into groups according to their common haloes. For completeness, we present a brief description of the group finder here, but refer the reader to Yang et al. (2004b) for details.

The halo-based group finder consists of the following main steps.

Step 1. Two different methods are combined to identify the centres (and members) of potential groups. First, we use the traditional FOF algorithm with very small linking lengths to assign galaxies into groups. The geometrical centres of all FOF groups thus identified with more than two galaxies are considered as centres of potential groups. Next, from all galaxies not yet linked together by these FOF groups, we select bright, relatively isolated galaxies which we also associate with the centres (and members) of potential groups.

Step 2. We estimate the luminosity of a selected potential group using

$$L_{\rm group} = \sum_i \frac{L_i}{f_{\rm c}(L_i)}, \tag{A1}$$

where L_i is the luminosity of each galaxy in the group, and $f_{\rm c}$ is the incompleteness of the survey. The total luminosity of the group is approximated by

$$L_{\rm total} = L_{\rm group} \frac{\int_0^\infty L\phi(L)\,{\rm d}L}{\int_{L_{\rm lim}}^\infty L\phi(L)\,{\rm d}L}, \tag{A2}$$

where $L_{\rm lim}$ is the minimum luminosity of a galaxy that can be observed at the redshift of the group, and $\phi(L)$ is the galaxy luminosity function.

Step 3. From $L_{\rm total}$ and a model for the group mass-to-light ratio, we compute an estimate of the halo mass associated with the group under consideration. From this estimate we also compute the halo radius r_{180}, the virial radius $r_{\rm vir}$ and the virial velocity $V_{\rm vir} = (GM/r_{\rm vir})^{1/2}$. The line-of-sight velocity dispersion of the galaxies within the dark matter halo is assumed to be $\sigma = V_{\rm vir}/\sqrt{2}$.

Step 4. Once we have a group centre, and a tentative estimate of the group size, mass and velocity dispersion, we can assign galaxies to this group according to the properties of the associated haloes. If we assume that the phase-space distribution of galaxies follows that of the dark matter particles, the number density contrast of galaxies in redshift space around the group centre (= centre of dark matter

halo) at redshift $z_{\rm group}$ can be written as

$$P_M(R,\,\Delta z) = \frac{H_0}{c}\,\frac{\Sigma(R)}{\bar{\rho}}\,p(\Delta z). \tag{A3}$$

Here $\Delta z = z - z_{\rm group}$ and $\Sigma(R)$ is the projected surface density of a (spherical) Navarro, Frenk & White (1997) halo, while the function $p(\Delta z)\,{\rm d}\Delta z$ describes the redshift distribution of galaxies within the halo. See Yang et al. (2004b) for the functional forms of $\Sigma(R)$ and $p(\Delta z)$ used.

Thus defined, $P_M(R,\,\Delta z)$ is the three-dimensional density contrast in redshift space. In order to decide whether a galaxy should be assigned to a particular group we proceed as follows. For each galaxy we loop over all groups, and compute the corresponding distance $(R,\Delta z)$ between galaxy and group centre. Here R is the projected distance at the redshift of the group. If $P_M(R,\Delta z) \geqslant B$, with $B = 10$ an appropriately chosen background level, the galaxy is assigned to the group. If a galaxy can be assigned to more than one group, it is only assigned to the group for which $P_M(R,\Delta\, z)$ has the highest value. Finally, if all members of two groups can be assigned to one group according to the above criterion, the two groups are merged into a single group.

Step 5. Using the group members thus selected we recompute the group-centre and go back to Step 2, iterating until there is no further change in the memberships of groups. Note that, unlike the traditional FOF method, this group finder also identifies groups with only one member.

A2 The assignment of L_{18} to groups

As discussed in Yang et al. (2004b), it is not reliable to estimate the (total) group luminosity based on the assumption that the galaxy luminosity function in groups is similar to that of field galaxies. Therefore, we used a more empirical approach to estimate the group luminosity L_{18}, defined as the total luminosity of all group members brighter than $M_{b_J} - 5\log h = -18$. The assignment of L_{18} to a group goes as follows.

(i) We estimate the group luminosity $L_{\rm group}$ with equation (A1) using only galaxies with $M_{b_J} - 5\log h \leqslant -18.0$.

(ii) We compute the absolute magnitude limit $M_{b_J,{\rm lim}} - 5\log h$ at the redshift of the group under consideration.

(iii) If $M_{b_J,{\rm lim}} - 5\log h \geqslant -18.0$, then we set $L_{18} = L_{\rm group}$; otherwise $L_{18} = L_{\rm group} \times f\,(L_{\rm group},\, M_{b_J,{\rm lim}})$, where $f\,(L_{\rm group},\, M_{b_J,{\rm lim}})$ is the correction factor determined from groups at lower redshifts where the galaxy sample is complete down to $M_{b_J} - 5\log h \leqslant -18.0$.

To determine the correction factor between $L_{\rm group}$ and L_{18} we first select *all* groups with $z \leqslant 0.09$, which corresponds to the redshift for which a galaxy with $M_{b_J} - 5\log h = -18$ has an apparent magnitude equal to the mean limiting magnitude of the 2dFGRS ($b_J \leqslant 19.3$). By applying further absolute magnitude limit cuts, we estimate $L_{\rm group}$ $(M_{b_J} \geqslant M_{b_J,{\rm cut}})$ and consider the ratio $L_{18}/L_{\rm group}$ as a function of $M_{b_J,{\rm cut}}$) (see fig. 9 in Yang et al. 2004b). We fit the $L_{18}/L_{\rm group} - M_{b_J,{\rm cut}}$ relation to a functional form $[\log(L_{\rm group}/a_0)]^{a_1\Delta M^2 + a_2\,\Delta M}$, where $\Delta M = M_{b_J,{\rm lim}} - 5\log h - 18.0$, by adjusting a_0, a_1 and a_2, and use this fit result as an estimate for the correction factor, $f\,(L_{\rm group},\, M_{b_J,{\rm lim}})$. Note that the correction factor obtained in this way is an average, and is not expected to be accurate for individual groups. However, as demonstrated in detail in Yang et al. (2004b), L_{18} so defined is quite tightly correlated with the mass of the dark matter halo hosting the group in the mock catalogue, and can be used to rank galaxy groups according to halo masses.

This paper has been typeset from a TEX/LATEX file prepared by the author.